



Robust streamlined two-dimensional offline coupling of asymmetrical flow field-flow fractionation and capillary electrophoresis for the separation and quantitation of a five-component submicron particle mixture

Meng Jing^{a,*}, Mingkang Sun^a, Wei Gao^a, Kathleen Michels^a, Rebecca Mort^a, Paul D. Hutchins^b

^a Analytical Science, Core R&D, The Dow Chemical Company, Collegeville, PA, 19426, United States

^b Analytical Science, Core R&D, The Dow Chemical Company, Midland, MI, 8640, United States

ARTICLE INFO

Keywords:

Asymmetrical flow field-flow fractionation
Capillary electrophoresis
Laser-induced fluorescence
Light scattering
Submicrometer particle

ABSTRACT

Characterization of submicrometer particles by size and surface charge is critical to understanding their property and functionality in industrial formulations. Although the recently reported offline coupling of asymmetrical flow field-flow fractionation and capillary electrophoresis (AF4×CE) shows success in separating a five-component submicrometer particle mixture based on size and mobility, it is a long and tedious process requiring extensive method development and instrument expertise. Moreover, it suffers from low throughput and ambiguity in large particle identification, limiting its widespread acceptance and application in industry. Here we report a new AF4×CE-laser-induced fluorescence (LIF) method which involves minimal method development and eliminates both the large sample injection and subsequent on-capillary stacking in CE separation, to significantly streamline separation and improve analysis throughput. Comprehensive characterization of eight fluorescently labeled five-component submicrometer particle mixture standards, at the concentration ratio of 200 : 200 : 133 : 133 : 334 and the total concentration level of 1000–10,000 mg/L, and a random sample can be performed within several days. In the lowest-concentration standard, as few as 2.97×10^2 particles at the peak center can be detected on the two-dimensional plot for the 500 nm particles, indicating extremely high detection sensitivity. By eliminating the overstacking issue, large particles can be unambiguously identified on the 2D plot based on the migration time. AF4-light scattering (LS) quantitation demonstrates good accuracy for the artificial five-component sample even when the five components are not completely separated. Moreover, AF4×CE-LIF quantitation is explored for future more challenging mixtures requiring higher separation capacity and resolution.

1. Introduction

Polymeric particles and polymeric nanocomposites in the size range of 1–1000 nm have various industrial applications, such as in packaging [1,2], cosmetics [3,4], pharmaceutical [5,6], foods [7], coatings [8,9], and water treatment [10,11]. The already large global market for polymeric nanoparticles is expected to grow rapidly in the next decade [12]. The synthesis, processing, functionalization, and formulation of nanoparticles cause significant complexity in their size distribution and surface properties, which are critical in application performance as well as regulation and safety measures [13]. Therefore, product development

requires simultaneous characterization of both size and mobility distributions for multi-component particle systems which has been a constant pursuit of industrial analytical chemists.

Recent technical developments for simultaneous size and mobility measurement include phase-analysis light scattering [14], carbon nanotube coulter counters [15], and suspended microchannel resonators [16]. However, these techniques either measure a weighted average rather than a distribution or need further improvements in instrument robustness to be commercially viable. Capillary Electrophoresis (CE) separates components based on electrophoretic mobility with extremely high separation efficiency [17,18] but is limited when used for particle

This article is part of a special issue entitled: Frontiers in electrophoresis published in Talanta.

* Corresponding author.

E-mail address: mjing@dow.com (M. Jing).

<https://doi.org/10.1016/j.talanta.2025.127816>

Received 15 November 2024; Received in revised form 13 February 2025; Accepted 24 February 2025

Available online 1 March 2025

0039-9140/© 2025 Elsevier B.V. All rights reserved, including those for text and data mining, AI training, and similar technologies.

analysis. The size and surface charge distributions are convoluted in CE separation, resulting in broad peaks. Recent work on coupling of CE with single-particle inductively coupled plasma-mass spectrometry (SP-ICP-MS) [19–21] and asymmetrical flow field-flow fractionation (AF4) [22–25] have demonstrated greatly improved separation resolution and intuitive characterization of both size and surface charge properties by deconvoluting size from mobility.

These advancements show significant resolving power for mixtures of particles equal to or smaller than 100 nm. However, characterization of complex particle mixtures larger than 100 nm, which are highly relevant to industrial nanoparticles and nanocomposites, remains challenging. Increased size and surface charge distributions require significantly expanded separation capacity and ultra-sensitive detection methods. Our recent work on offline coupling of AF4 and CE demonstrated the successful separation of a five-component submicron particle mixture consisting of 50, 100, 200, 300, and 400 nm polystyrene (PS) particles [26]. An on-capillary enrichment method using reversed electrode polarity stacking mode (REPSM) was developed to concentrate particles for ultraviolet detection. Although this work enables submicrometer colloidal particles characterization, several drawbacks restrain the AF4×CE from being a robust separation platform. First, the REPSM stacking requires very careful method development to identify the appropriate resistivity ratio of background electrolyte (BGE) and sample zone, sample injection plug length, and stacking voltage and time. Additionally, the extended analysis time (12.3 min for each fraction), significantly increases the overall AF4×CE analysis time. Moreover, the on-capillary stacking can cause mild particle interactions and overstacking, especially for large particles [27]. We observed earlier migrations for the 400 nm particles which resulted in reduced resolution of the 300–400 nm pair compared to one-dimensional (1D) CE separation. The change in mobility also complicated locating the 400 nm particles in the final two-dimensional (2D) contour plot, as the elution/migration time is the most important reference in identification. Due to these challenges, we did not explore particles larger than 400 nm.

In this manuscript, we report a robust, streamlined AF4×CE method with minimal method development, elimination of on-capillary REPSM stacking, and reduction of injection time from 160 s to 5 s by fluorescently labeling the five-component submicrometer PS particle mixture in approximately the same size range (50–500 nm). Fluorescent tags greatly improve detection limits, removing need for REPSM which could generate elution/migration times that cannot be correlated to 1D separation. We further cut the total number of fractions by half with no loss of separation resolution relative to either AF4 or CE dimension. This AF4×CE-LIF platform demonstrates superior separation due to improved peak capacity and resolution compared to either dimension with minimum (AF4) or no (CE) 1D method development, a huge advantage compared to existing 1D separation approaches [28]. Since the overall AF4×CE-laser-induced fluorescence (LIF) analysis time has been reduced by 75 %, five-component particle mixtures prepared at eight different concentrations can be analyzed in a few days to create the calibration curve, which is then applied for the determination of concentrations of each individual particle components in an artificially prepared “unknown” particle mixture with high accuracy.

2. Experimental procedures

2.1. Chemicals

The Fluoresbrite YG Microsphere Series at 50 nm, 100 nm, 200 nm, 300 nm, and 500 nm (catalog number: 16661-10, 17150-10, 17151-10, 24051-10, and 17152-10, respectively) were purchased from Polysciences (Warrington, PA USA) at approximately 2.6 % by weight. Size distributions of these particles were at 10 %, 5 %, 4 %, and 3 % coefficient of variation, for 50 nm, 100 nm, 200 nm, 300 nm, and 500 nm particles respectively. The excitation maximum was at 441 nm, the emission maximum was at 486 nm, and the fluorescent spectra of these

particles were similar to that of fluorescein isothiocyanate (FITC) dye according to the manufacturer. These particles were stored at 4 °C in darkness at the original concentration. Before use, mild shaking was performed for 30 s followed by dilution in Milli-Q water (from a Milli-Q® IQ 7000 Ultrapure Lab Water System, MilliporeSigma, Burlington, MA USA) or a low conductivity BGE prepared in Milli-Q water. HPLC grade toluene (T291SK-4) and Fisherbrand™ FL-70™ concentrate (catalog number: SF105-1) were purchased from Fisher Scientific (Hampton, NH USA). Boric acid (catalog number: B7901) was purchased from Sigma-Aldrich (St. Louis, MO USA). The mobile phase of AF4 was prepared by diluting the FL-70™ concentrate in Milli-Q water by 1000-fold and disposed of every two weeks. The BGE of CE was prepared by dissolving 100 mM boric acid in Milli-Q water and pH adjusted to 9.2 with 1 M sodium hydroxide solution. This buffer was stored at 4 °C up to 30 days and used freshly to a desired lower concentration for daily use.

2.2. Instruments

The AF4 separation channel was between 0.3 cm and 2.15 cm in width and 19.5 cm in length with a 350 µm-thick spacer. The membrane used was a regenerated cellulose membrane with a 10 kDa MW cutoff (Wyatt Technology Corp., Santa Barbara, CA USA). An Eclipse™ Dual-Tec system from Wyatt Technology was applied for regulating the AF4 flow. An Agilent 1200 series isocratic pump equipped with a micro-vacuum degasser (Agilent Technologies, Santa Clara, CA USA) was employed to deliver the flow. An Agilent 1200 series autosampler was used for all injections. A DAWN HELOS II multi-angle laser light scattering detector (MALS) from Wyatt Technology was calibrated by toluene and the 90-degree MALS detector was used to collect data at 1 Hz. An Agilent 1260 fraction collector was used to collect the effluent from AF4 every minute for subsequent CE analysis. The optimized AF4 method used for sample fractionation was established with the detector flow of 0.6 mL/min, injection flow of 0.2 mL/min, and other details in Supplementary Material (Table S1). Fraction collection started at 14.0 min of the separation and was at the frequency of one collection per minute. The collected 35 fractions were then analyzed on CE without further enrichment. To estimate the concentration of particles after AF4 fraction collection, a Wyatt OptiLab T-rEX refractive index (RI) detector was used to replace the Agilent 1260 fraction collector in the AF4 system. All AF4 data were collected and processed using the Astra 8.1.2.1 software (Wyatt Technology Corp.).

A SCIEX CESI 8000 Plus system (AB Sciex LLC, Framingham, MA USA) equipped with a solid-state laser induced fluorescence (LIF) detector at 488 nm was used to perform all the CE experiments. A fresh bare fused-silica (BFS) capillary with polyimide external coating (60 cm long, 75 µm inner diameter, Agilent Technologies, catalog number 160-2644-5) was trimmed to fit into a standard cartridge. The LIF detector was set in direct detection mode at the excitation wavelength of 488 nm and emission wavelength of 520 nm with a data rate of 4 Hz. Both the capillary cartridge and sample storage temperatures were set at 25 °C. The fresh BFS capillary was conditioned with 1 M NaOH at 50 psi for 5 min, followed by Milli-Q water at 50 psi for 5 min, and then BGE at 50 psi for 5 min. The new capillary was then stored in BGE for over 24 h to fully condition the inner surface before being used for separation. A 0.1 M NaOH rinse at 50 psi for 1 min followed by BGE rinse at 50 psi for 1 min was applied before each injection of sample. AF4 fractions were pressure injected at 0.5 psi for 5 s, and the separation was performed by applying 30 kV voltage in normal polarity mode for 15 min.

2.3. Data processing

Individual CE-LIF data files were extracted and processed using an in-house program written in Java (JRE 1.8). The details for data extraction and compilation, baseline correction, and data conversion source code can be found in the Supplementary Material of a previous publication.²⁶ The resulting Excel files were imported into JMP Pro

17.0.0 to obtain contour plots and imported into LC Image 2.8r3.1 for peak integration and 2D quantitation.

3. Results and discussion

3.1. AF4×CE characterization of a five-component 50–500 nm submicron particle mixture

The AF4 setup and timetable (Table S1) were largely similar to the previous publication [26]. An exponential gradient of the crossflow rate allowed baseline separation of the 50–100 nm pair (Fig. 1A), and the following linear elution at a reduced cross flow rate was applied for larger particles. The only differences were that the cross flow rate was reduced to 0.25 mL/min rather than 0.30 mL/min at the end of the exponential gradient, and the linear elution was kept for 20 min compared to 16 min in the previous method. These two changes allowed for a shallower gradient in the linear elution region and slightly improved separation of the large particles (200/300/500 nm). Although not completely resolved, these three particle distributions have partial separation as evidenced by distinct peak apexes in Fig. 1A. The overall AF4 separation time was slightly longer resulting in a slightly larger dilution factor. This proved not to be an issue since the fluorescent tagging allows much more sensitive detection in the second dimension (²D) separation. It should be noted that these very minor modifications of the ¹D AF4 method were achieved based on the previously published method [26] within only a few hours of method development.

The CE method was identical to our previous publication in terms of BGE and separation conditions [26], but a much shorter injection (0.5 psi × 5 s) was applied to replace the long injection of 0.5 psi × 160 s for on-capillary stacking. This change significantly reduced the complexity of implementation and the overall method time. Fig. 1B shows the complex CE electropherograms of the five Fluoresbrite YG Microspheres samples marked by heavy coelution: the 50–100 nm pair and the 200–300 nm pair both have coelution issue, and the 500 nm distribution although mainly separated from the previous two groups still has minor components overlapping with the other particle distributions. These results are not surprising since CE separation is based on both particle size and surface charge, and these Fluoresbrite YG Microspheres may have different surface charges and/or charge densities.

As shown in Fig. 1C, the 50–100 nm pair is resolved in both the AF4×CE and AF4 separation (Fig. 1A). Similarly, the 200–300 nm pair is partially resolved in AF4×CE as they are by AF4. The 500 nm particles that cannot be completely resolved from other particles by either AF4

(Fig. 1A) or CE (Fig. 1B) separation can now be much better separated by AF4×CE (Fig. 1C). Two smears are observed (red circles in Fig. 1C), which extend into smaller size (smear 1) and into earlier electrophoretic mobility (smear 2), suggesting different particle populations. This result further proves the separation power and characterization advantages of AF4×CE as neither single dimension can clearly map out these two different populations. It is also important to point out that both the CE migration time and AF4 fraction number on the 2D plot (Fig. 1C) remain unchanged for all five particle distributions from 50 nm to 500 nm. This result proves that the AF4 mobile phase, focusing, and separation steps do not destabilize or modify the particles. Our previous best separation [26] showing decreased migration time of the 400 nm particles was probably due to on-capillary stacking. To our best knowledge, this is the first time that five-component particle mixtures over one order of size magnitude (50–500 nm) were separated with unambiguous identification in any AF4×CE separation. For PS particles separation, previous 1D CE methods were developed to separate different size and surface charges; however, extensive research was required to characterize particle zeta potential and optimize CE conditions such as the type, pH, and concentration of BGE, separation voltages, and additives [28]. Here we demonstrate the great advantage of performing AF4×CE - different separation mechanisms on the two dimensions significantly improved the overall separation peak capacity and resolution compared to either dimension and therefore tedious scrutinizing CE separation conditions to optimize one dimensional separation is not necessary.

To estimate the concentration of particles at their peak AF4 elution time, an RI detector was added to the AF4 system (Fig. S1) to estimate the peak apex concentration for each particle distribution. Taking the 1000 mg/L mixture (in Fig. 1) for example, the results are shown in Table S2 with the peak concentrations in the range of 0.216–0.814 mg/L. When analyzed on CE only 25.1 nL of sample was injected based on calculations from the 0.5 psi × 5 s injection and the Hagen-Poiseuille equation [29]. Therefore, these peak apex fractions correspond to approximately 1.64×10^5 , 3.04×10^4 , 1.23×10^3 , 5.53×10^2 , and 2.97×10^2 particles injected on capillary for 50, 100, 200, 300, and 500 nm, respectively (see Table S3 for more details on calculation). Other fractions from AF4 had even fewer particles injected on ²D CE. Therefore, with fluorescent tagging, the 2D AF4×CE-LIF results demonstrate extremely sensitive detection, down to hundreds of particles per fraction or thousands of particles per size population, comparable to results obtained from some of the most sensitive quantitative detection techniques such as ICP-MS [19–21,30] and flowcytometry [31].

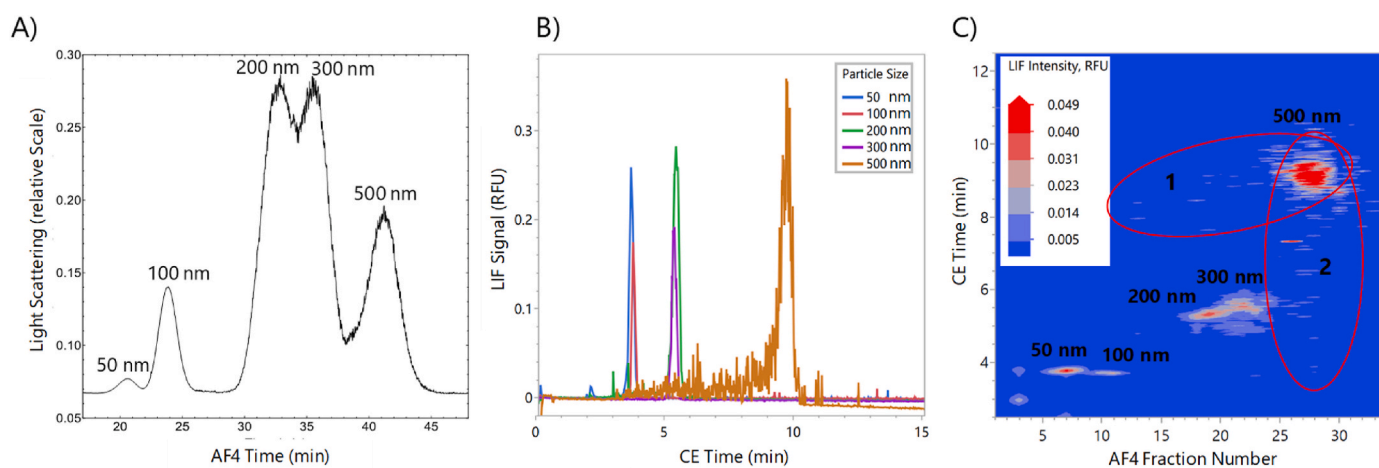


Fig. 1. (A) AF4 fractogram of the 50 nm, 100 nm, 200 nm, 300 nm, and 500 nm Fluoresbrite YG Microsphere mixture at the mass ratio of 200:200:133:133:334 with a total level of 1000 mg/L and injection volume of 4 μ L, detected by light scattering at 90°, (B) CE electropherogram overlay of individual injections of 50 nm, 100 nm, 200 nm, 300 nm, and 500 nm Fluoresbrite YG Microspheres at 5 mg/L by hydrodynamic injection (0.5 psi × 5 s), and (C) AF4×CE 2D contour plot of the AF4 fractions collected from (A).

3.2. 1D quantitation by AF4-LS

To evaluate determination of particle distribution concentration, we first explored quantitative performance for the 1D AF4 using a LS detector. Since the intensity of scattered light at a fixed angle for the same species only depends on its concentration, height or area of the LS peak was explored for concentration determination [32]. First, a series of calibration standards containing the same mass ratio of the five components but at different concentrations were prepared. The total concentrations of this sample series range from approximately 1000 mg/L to 10,000 mg/L, with a mass ratio of 200: 200: 133: 133: 334 for 50 nm: 100 nm: 200 nm: 300 nm: 500 nm microspheres. An apex for each component was identifiable based on the AF4 fractogram (Fig. 2A), despite insufficient separation between different components. Then, calibration curves for peak heights against nine microsphere concentrations were established for all five components with good linear correlations and all R^2 values greater than 0.99 (Fig. 3). Next, to simulate a more realistic experimental scenario, five random concentrations were generated by applying random generator function in Excel between 0 and 1, and these five numbers were multiplied by the calibration concentration range to obtain random concentrations for individual microsphere distributions (shown in Table 1). AF4 separation using the same setup and flow program showed that all five components eluted at the same elution time of the calibration standards (Fig. 2B). Peak height values for each component in the artificial sample were measured in triplicate, which were then used to calculate the concentration of each microsphere distribution based on the calibration curves. As shown in Fig. 2B (red dots) and Table 1, decent accuracies were achieved,

validating this quantitation method. Besides peak heights, similar quantitation using peak areas was also attempted (Fig. S2 and Table S4). Slightly worse linearity and accuracy were found for the peak area method, likely due to the overlap between peaks that interfered with the determination of peak boundaries. It is worth pointing out that although clear peak apexes were expected critical for the AF4-LS quantitation, satisfactory results were still obtained for the challenging 200–300 nm pair with significantly different concentrations.

3.3. Attempts at 2D quantitation by AF4×CE - LIF

Since 2D AF4×CE separation greatly improves peak capacity and separation resolution, and LIF enables highly sensitive detection, we also explored quantitation on the 2D analysis. Integration and data processing were performed in the LC Image software. As shown in Fig. 4, the 200 nm (blob 1) and 300 nm (blob 2) particle populations in the artificial sample can be better resolved on the 2D plot compared to 1D AF4 (Fig. 2B) when the concentrations are significantly different. Theoretically, the 2D peak volume function (results shown in Table S5) allows integration of the identified blob using the smoothed signals from multiple AF4 fractions. By constructing the calibration curve from aforementioned standards, the unknown level of 200 nm particles in the artificial sample should be more confidently determined as compared to 1D AF4 in which the 200 nm and 300 nm particles were not well resolved (Fig. 2A). However, in reality we observed worse linearity; moreover, the accuracy of the random sample were not comparable to those obtained from LS (data not shown).

In order to understand poor quantitative performance, Fluoresbrite YG Microspheres were prepared in 0.1 % FL-70 at 5 mg/L individually and measured under the same 2D CE conditions repeatedly over roughly three days, mimicking the process these microspheres underwent for fractionation and CE measurement in the AF4×CE experiment. Taking the 100 nm and 300 nm microspheres as two individual examples monitored separately (Fig. 5), not surprisingly, large variations in peak area were observed. The 100 nm microspheres show some variance with the maximum/minimum signal ratio of 2.2; while the 300 nm microspheres have an increasing trend with the maximum/minimum signal ratio of 3.2. Both samples were prepared at 1.5 mL and the volume reduction after 3 days were within 100 μ L, so these changes were not due to increase in sample concentration from evaporation. Other conditions such as autosampler and cartridge temperatures, separation buffer vials, and the CE method were all kept the same. Future work will be focused on understanding if increasing capillary inner diameter or reducing laser power would help reduce the LIF power density to improve photostability [33]; if the AF4 mobile phases play a role in the re-distribution or quantum yield of the fluorescent tags embedded in these particles [34], other AF4 mobile phase options and both commercial and in-house chemical labeling of fluorescent tags on the surface of particles will be explored. If the fluorescent stability issue can be resolved, 2D AF4×CE-LIF will enable critical pair quantitation that is potentially very challenging by either one dimensional separation.

4. Conclusions

We demonstrate herein a robust, streamlined AF4×CE-LIF method for fast separation and unambiguous identification of a fluorescently tagged five-component submicrometer PS particle mixture in the size range of 50–500 nm without compromising separation resolution. The fluorescent labels and LIF detection allowed the elimination of large volume injection on CE and the on-capillary stacking, significantly improving analysis throughput so that nine calibration standards and three injections of a randomly made artificial sample can be analyzed within several days. This approach also successfully solved the issue of varying migration time on 2D plot due to overstacking. Particles as large as 500 nm can be readily identified. AF4-LS quantitation was performed on the artificial sample, and the five components were quantified with

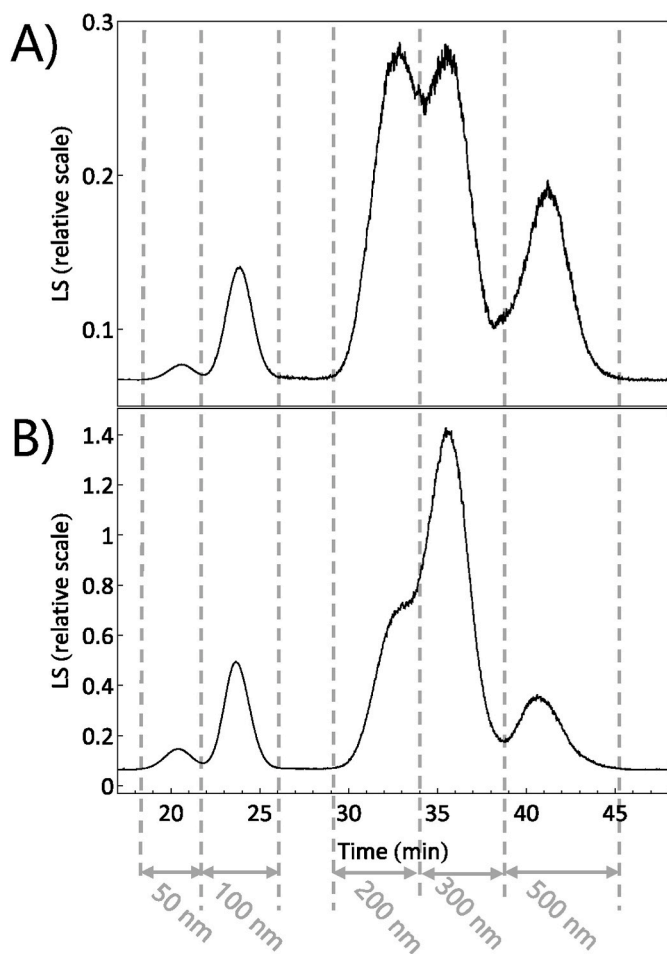


Fig. 2. AF4 fractogram with MALS detection at 90° for (A) a representative calibration standard and (B) the artificial sample.

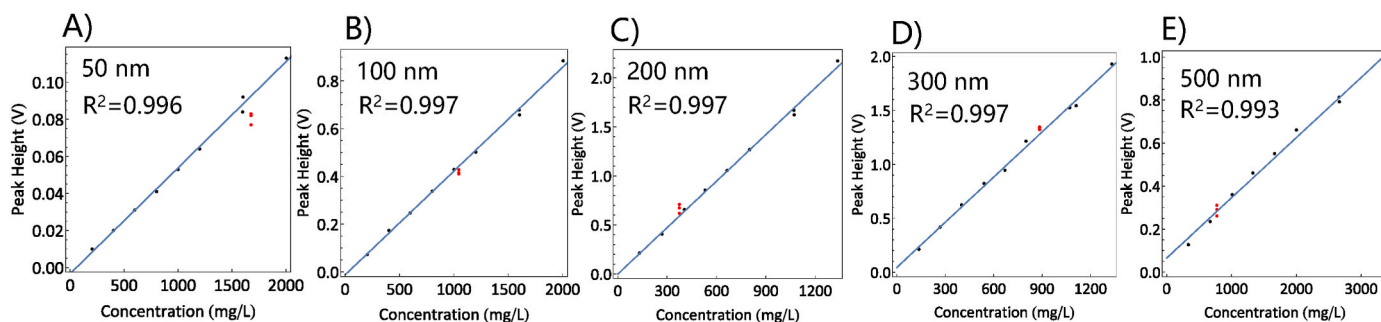


Fig. 3. Calibration curves of (A) 50 nm, (B) 100 nm, (C) 200 nm, (D) 300 nm, and (E) 500 nm PS microspheres constructed from nine five-component standards (black dots) based on LS peak heights and quantitation of individual components in the artificial sample (red dots). Blue lines are the linear calibration curves with R^2 values indicated on the plot. (For interpretation of the references to colour in this figure legend, the reader is referred to the Web version of this article.)

Table 1

Quantitative measurement of the concentration of microspheres at different sizes for the artificial five-component sample based on peak heights.

Particle size	50 nm	100 nm	200 nm	300 nm	500 nm
Theoretical concentration (mg/L)	1677	1045	374	884	774
Mean and standard deviation of measured concentration (mg/L)	1473 ± 56	988 ± 20	417 ± 29	926 ± 9	792 ± 90
Relative standard deviation (%)	3.8	2.0	7.0	1.0	11
Accuracy range (%)	84–89	93–97	103–118	104–106	90–113

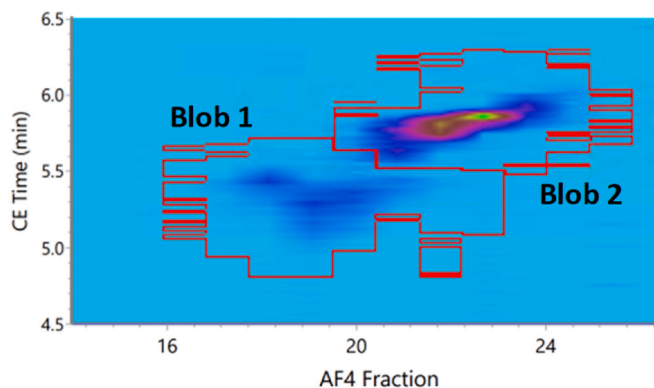


Fig. 4. Blob identification of the 200 nm (blob 1) and 300 nm (blob 2) particles in the random artificial five-component sample.

good accuracy. Two-dimensional AF4×CE-LIF quantitation was also explored for future more challenging mixtures whose quantitation might require higher separation capacity and resolution. Despite the challenge of unstable fluorescence intensity encountered in 2D quantitation, we have examined experimental conditions and developed with hypotheses for future explorations. These include increasing the capillary inner diameter, reducing laser power, exploring different buffer options, and chemically labeling of fluorescent tags on the surface of particles. With these advancements in the AF4×CE platform for particle analysis, future work can be expanded to a wider size range such as 100 nm - 10 μm, which has broader interest in pharmaceutical industries [35] and environmental research [36]. AF4 is known for matrix cleaning capable of removing small-molecular-weight species such as salts and surfactants. For AF4 separation, a mixture consisting of nanometer, submicrometer, and micrometer particles would go beyond the normal mode and separation occurs under both normal mode and steric mode separation mechanisms [37], meaning reversed elution pattern for micrometer

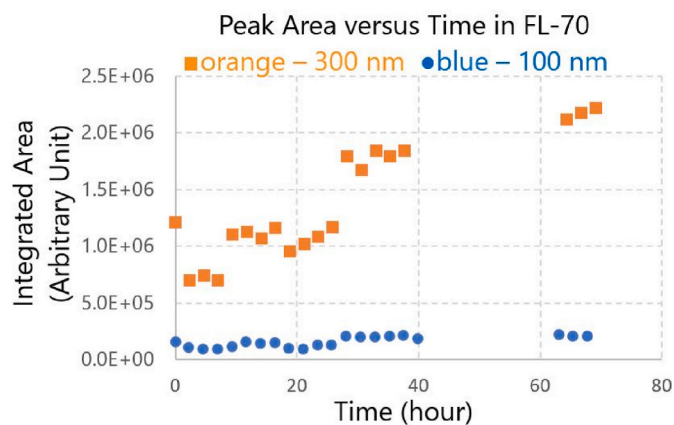


Fig. 5. Fluorescence signal stability over roughly three days for the 5 mg/L 100 nm and 300 nm Fluoresbrite YG Microspheres analyzed under the same 2D CE conditions.

particles and coelution of small and large particles in a particular fraction collection. However, since the 2D CE separation is based on electrophoretic mobility, this AF4×CE platform would potentially allow complete separation of such challenging particle mixtures in a wide size range with high peak capacity and resolution and minimal influence from sample matrix.

CRediT authorship contribution statement

Meng Jing: Writing – review & editing, Writing – original draft, Validation, Methodology, Investigation, Funding acquisition, Formal analysis, Data curation, Conceptualization. **Mingkang Sun:** Writing – review & editing, Writing – original draft, Methodology, Investigation, Formal analysis, Data curation, Conceptualization. **Wei Gao:** Writing – review & editing, Software, Methodology, Conceptualization. **Kathleen Michels:** Methodology, Data curation. **Rebecca Mort:** Writing – review & editing, Methodology, Data curation. **Paul D. Hutchins:** Writing – review & editing, Methodology, Investigation, Formal analysis.

Declaration of competing interest

The authors declare the following financial interests/personal relationships which may be considered as potential competing interests: Meng Jing reports financial support was provided by The Dow Chemical Company. If there are other authors, they declare that they have no known competing financial interests or personal relationships that could have appeared to influence the work reported in this paper.

Acknowledgements

The authors gratefully acknowledge Dr. James Bohling for valuable technical discussion and Dr. Junsu Gu for reviewing the manuscript, and The Dow Chemical Company for funding this work.

Appendix A. Supplementary data

Supplementary data to this article can be found online at <https://doi.org/10.1016/j.talanta.2025.127816>.

Data availability

Data will be made available on request.

References

- [1] A. Bratovic, A. Odobasic, S. Catic, I. Sestan, Application of polymer nanocomposite materials in food packaging, *Croat. J. Food Sci. Technol.* 7 (2015) 86–94, <https://doi.org/10.17508/CJFST.2015.7.2.06>.
- [2] C. Vasile, Polymeric nanocomposites and nanocoatings for food packaging: a review, *Mater. (Basel, Switz.)* 11 (2018) 1834–1882, <https://doi.org/10.3390/ma11101834>.
- [3] N. Popadyuk, A. Popadyuk, A. Kohut, A. Voronov, Thermoresponsive latexes for fragrance encapsulation and release, *Int. J. Cosmet. Sci.* 38 (2016) 139–147, <https://doi.org/10.1111/ics.12267>.
- [4] L. Xu, Y. Zhou, S. Amin, *Polymer Colloids for Cosmetics and Personal Care*, Royal Society of Chemistry, London, UK, 2019.
- [5] F. Molavi, M. Barzegar-Jalali, H. Hamishehkar, Polyester based polymeric nano and microparticles for pharmaceutical purposes: a review on formulation approaches, *J. Contr. Release* 320 (2020) 265–282, <https://doi.org/10.1016/j.jconrel.2020.01.028>.
- [6] K.M. El-Say, H.S. El-Sawy, Polymeric nanoparticles: promising platform for drug delivery, *Int. J. Pharm.* 528 (2017) 675–691, <https://doi.org/10.1016/j.ijpharm.2017.06.052>.
- [7] D.J. McClements, The future of food colloids: next-generation nanoparticle delivery systems, *Curr. Opin. Colloid Interface Sci.* 28 (2017) 7–14, <https://doi.org/10.1016/j.cocis.2016.12.002>.
- [8] W. Wichaita, D. Polpanich, P. Tangboriboonrat, Review on synthesis of colloidal hollow particles and their applications, *Ind. Eng. Chem. Res.* 58 (2019) 20880–20901, <https://doi.org/10.1021/acs.iecr.9b02330>.
- [9] S. Jiang, A.V. Dyk, A. Maurice, J. Bohling, D. Fasano, S. Brownell, Design colloidal particle morphology and self-assembly for coating applications, *Chem. Soc. Rev.* 46 (2017) 3792–3807, <https://doi.org/10.1039/C6CS00807K>.
- [10] K. Ahmad Momina, Study of different polymer nanocomposites and their pollutant removal efficiency: review, *Polymer* 217 (2021) 123453–123475, <https://doi.org/10.1016/j.polymer.2021.123453>.
- [11] J. Tripathy, A. Mishra, M. Pandey, R.R. Thakur, S. Chand, P.R. Rout, M.K. Shahid, Advances in nanoparticles and nanocomposites for water and wastewater treatment: a review, *Water* 16 (2024) 1481–1506, <https://doi.org/10.3390/w16111481>.
- [12] Global polymeric nanoparticles market by type, by application, by geographic scope and forecast, <https://www.verifiedmarketreports.com/product/polymeric-nanoparticles-market/>, 2025.
- [13] W.J. Stark, P.R. Stoessel, W. Wohlleben, A. Hafner, Industrial applications of nanoparticles, *Chem. Soc. Rev.* 44 (2015) 5793–5805, <https://doi.org/10.1039/C4CS00362D>.
- [14] F. McNeil-Watson, W. Tscharnuter, J. Miller, A new instrument for the measurement of very small electrophoretic mobilities using phase analysis light scattering (PALS), *Colloids Surf. A Physicochem. Eng. Asp.* 140 (1998) 53–57, [https://doi.org/10.1016/S0927-7757\(97\)00267-7](https://doi.org/10.1016/S0927-7757(97)00267-7).
- [15] T. Ito, L. Sun, R.R. Henriquez, R.M. Crooks, A carbon nanotube-based coulter nanoparticle counter, *Acc. Chem. Res.* 37 (2004) 937–945, <https://doi.org/10.1021/ar040108+>.
- [16] P. Dextras, T.P. Burg, S.R. Manalis, Integrated measurement of the mass and surface charge of discrete microparticles using a suspended microchannel resonator, *Anal. Chem.* 81 (2009) 4517–4523, <https://doi.org/10.1021/ac9005149>.
- [17] J.W. Jorgenson, K.D. Lukacs, K. D. Zone, Electrophoresis in open-tubular glass capillaries, *Anal. Chem.* 53 (1981) 1298–1302, <https://doi.org/10.1021/ac00231a037>.
- [18] N.W. Frost, M. Jing, M.T. Bowser, M.T. Capillary Electrophoresis, *Anal. Chem.* 82 (2010) 4682–4698, <https://doi.org/10.1021/ac101151k>.
- [19] D. Mozhayeva, D.C. Engelhard, Separation of silver nanoparticles with different coatings by capillary electrophoresis coupled to ICP-MS in single particle mode, *Anal. Chem.* 89 (2017) 9767–9774, <https://doi.org/10.1021/acs.analchem.7b01626>.
- [20] D. Mozhayeva, I. Strenge, C. Engelhard, Implementation of online preconcentration and microsecond time resolution to capillary electrophoresis single particle inductively coupled plasma mass spectrometry (CE-SP-ICP-MS) and its application in silver nanoparticle analysis, *Anal. Chem.* 89 (2017) 7152–7159, <https://doi.org/10.1021/acs.analchem.7b01185>.
- [21] B. Franze, I. Strenge, C. Engelhard, Separation and detection of gold nanoparticles with capillary electrophoresis and ICP-MS in single particle mode (CE-SP-ICP-MS), *J. Anal. At. Spectrom.* 32 (2017) 1481–1489, <https://doi.org/10.1039/C7JA00040E>.
- [22] Z. You, N. Jakubowski, U. Panne, S.M. Weidner, Separation of polystyrene nanoparticles with different coatings using two-dimensional off-line coupling of asymmetrical flow field flow fractionation and capillary electrophoresis, *J. Chromatogr. A* 1593 (2019) 119–126, <https://doi.org/10.1016/j.chroma.2019.01.056>.
- [23] Z. You, N. Nirmalanathan-Budau, U. Resch-Genger, U. Panne, S.M. Weidner, Separation of polystyrene nanoparticles bearing different carboxyl group densities and functional groups quantification with capillary electrophoresis and asymmetrical flow field flow fractionation, *J. Chromatogr. A* 1626 (2020) 461392–461399, <https://doi.org/10.1016/j.chroma.2020.461392>.
- [24] Z. Gao, Z. Hutchins, Z. Li, W. Zhong, Offline coupling of asymmetrical flow field-flow fractionation and capillary electrophoresis for separation of extracellular vesicles, *Anal. Chem.* 94 (2022) 14083–14091, <https://doi.org/10.1021/acs.analchem.2c03550>.
- [25] Z. Gao, Z. Li, Z. Hutchins, Q. Zhang, W. Zhong, Enhancing extracellular vesicle analysis by integration of large-volume sample stacking in capillary electrophoresis with asymmetrical flow field-flow fractionation, *Anal. Chem.* 95 (2023) 15778–15785, <https://doi.org/10.1021/acs.analchem.3c03303>.
- [26] M. Jing, W. Gao, P. Hutchins, Development of two-dimensional offline coupling of asymmetrical flow field-flow fractionation and capillary electrophoresis for the separation of a five-component submicrometer particle mixture, *Anal. Chem.* 95 (2023) 3840–3847, <https://doi.org/10.1021/acs.analchem.2c05352>.
- [27] L. Yu, S.F.Y. Li, Large-volume sample stacking with polarity switching for the analysis of bacteria by capillary electrophoresis with laser-induced fluorescence detection, *J. Chromatogr. A* 1161 (2007) 308–313, <https://doi.org/10.1016/j.chroma.2007.05.067>.
- [28] M.A. Caprise, A.C. Quevedo, K.R. Riley, Quantitative separation of polystyrene nanoparticles in environmental matrices with picogram detection limits using capillary electrophoresis, *Chem. Commun.* 60 (2023) 63–66, <https://doi.org/10.1039/D3CC04588A>.
- [29] E.T. da Costa, C.L. do Lago, Improving hydrodynamic injection in capillary electrophoresis by using the integral of pressure, *Electrophoresis* 45 (2024) 609–617, <https://doi.org/10.1002/elps.202300242>.
- [30] D. Ojeda, E. Bolea, J. Pérez-Arantegui, F. Laborda, Exploring the boundaries in the analysis of large particles by single particle inductively coupled plasma mass spectrometry: application to nanoclays, *J. Anal. At. Spectrom.* 37 (2022) 1501–1511, <https://doi.org/10.1039/D2JA00026A>.
- [31] A. Salvati, I. Nelissen, A. Haase, C. Aberg, S. Moya, A. Jacob, F. Alnasser, T. Bewersdorff, S. Deville, A. Luch, K.A. Dawson, Quantitative measurement of nanoparticle uptake by flow cytometry illustrated by an interlaboratory comparison of the uptake of labelled polystyrene nanoparticles, *NanoImpact* 9 (2018) 42–50, <https://doi.org/10.1016/j.impact.2017.10.004>.
- [32] W. Gao, J. Cohen, F. Acholla, W. Su, Recent progress in separation of macromolecules and particulates, *ACS Symp. Ser.* 1281 (2018) 111–143, <https://doi.org/10.1021/bk-2018-1281.ch007>.
- [33] V.A. Galievsky, A.S. Stasheuski, S.N. Krylov, “Getting the best sensitivity from on-capillary fluorescence detection in capillary electrophoresis” – a tutorial, *Anal. Chim. Acta* 935 (2016) 58–81, <https://doi.org/10.1016/j.aca.2016.06.015>.
- [34] G. Bastiat, C.O. Pritz, C. Roider, F. Fouchet, E. Lignieres, A. Jesacher, R. Glueckert, M. Ritsch-Marte, A. Schrott-Fischer, P. Saulnier, J.P. Benoit, A new tool to ensure the fluorescent dye labeling stability of nanocarriers: a real challenge for fluorescence imaging, *J. Contr. Release* 170 (2013) 334–342, <https://doi.org/10.1016/j.jconrel.2013.06.014>.
- [35] R.Y.P. da Silva, D.L.B. de Menezes, V. da S. Oliveira, A. Converti, A.A.N. de Lima, Microparticles in the development and improvement of pharmaceutical formulations: an analysis of in vitro and in vivo studies, *Int. J. Mol. Sci.* 24 (2023) 5441–5465, <https://doi.org/10.3390/ijms24065441>.
- [36] K. Ziani, C.B. Ionita-Mindrican, M. Mititelu, S.M. Neacsu, C. Negrei, E. Morosan, D. Draganescu, O.T. Preda, Microplastics: a real global threat for environment and food safety: a state of the art review, *Nutrients* 15 (2023) 617–650, <https://doi.org/10.3390/nu15030617>.
- [37] H. Dou, Y.J. Lee, E.C. Jung, B.C. Lee, S. Lee, Study on steric transition in asymmetrical flow field-flow fractionation and application to characterization of high-energy material, *J. Chromatogr. A* 1304 (2013) 211–219, <https://doi.org/10.1016/j.chroma.2013.06.051>.